magnitude of the bleach of D when the electric polarization vector of the 870-nm light is at an angle η to $\vec{H}$ is measured as a function of field, and its ratio with the value at zero field defines the relative yield, $I(H,\eta)$. We define a new quantity, the "quantum yield anisotropy", $a(H)$, as

$$a(H) = \frac{I(H,0°) - I(H,90°)}{I(H,0°) + 2I(H,90°)} \quad (1)$$

$I(H,0°)$ and $I(H,90°)$ for a viscous solvent are plotted in Figure 2A; $a(H)$ is plotted in Figure 2B for viscous and nonviscous solvents.[4] The dependence of $a(H)$ on viscosity is simply a consequence of the decay of $a(H)$ due to rotation on the time scale of its measurement, and the observation that $a(H) = 0.00 \pm 0.009$ for a nonviscous solution provides an excellent experimental control.[5]

A quantitative analysis of these data depends on the magnitude of each tensor quantity and its geometric relationship with the direction defined by the transition moment at 870 nm. The remarkable observation that the *sign* of $a(H)$ changes on going from low to high magnetic field implies that there are two or more anisotropic magnetic interactions contributing to $a(H)$. The field dependence of $a(H)$ is due to the *difference* **g** tensor between $D^{+}\cdot$ and $A^{-}\cdot$, while the anisotropy at low field (e.g., 1 kG) is due to the electron–electron and electron–nuclear dipolar tensors. The latter tensors need not be related in magnitude or relative orientation to the *difference* **g** tensor. Also note that $a(H)$ is essentially indpendent of field for fields >40 kG. At extremely high fields we expect the rate of the singlet–triplet mixing to exceed the recombination rate constants (Figure 1) for all orientations in the field. Consequently, the yield would be independent of the mixing rate and orientation, and $a(H)$ would equal zero; i.e., the observed $a(H)$ at 50 kG in Figure 2B is approximately at a turning point.[6]

We have previously derived a theoretical expression for the triplet quantum yield as a function of applied magnetic-field strength considering only isotropic magnetic interactions.[7] This expression is readily generalized for the case of both isotropic and anisotropic interactions; the formalism and details of actual calculations are presented elsewhere.[8] It is found that the anisotropic quantum yield data of Figure 2B can be fit with reasonable values for the anisotropic parameters, placing some limits on RC structures. EPR experiments on trapped, photoselected intermediates ($D^{+}\cdot$, $A^{-}\cdot$, and $D^{+}\cdot A^{-}\cdot$) are currently being performed, and these should augment the $a(H)$ data and allow the determination of several key structural features of the RC.

The new result demonstrated in Figure 2 is that *the yield of a chemical reaction involving radical pairs can depend on the orientation of the reactants in a magnetic field.* This is a natural consequence of the anisotropy of magnetic terms that drive or impede singlet–triplet mixing. This effect can be exploited to probe both magnetic properties of the radicals and structural properties of the short-lived radical pair itself, as the effect depends on the *difference* **g** tensor at high field. Although isotropic magnetic field effects on radical-pair reactions are well-known[9] and entirely predictable based on the CIDNP literature,[10] anisotropic magnetic-field effects have not been reported previously.[11] This is because radical-pair reactions are ordinarily studied in nonviscous solution, where molecular motion leads to a rapid loss of interradical interactions or rotational averaging of anisotropic magnetic terms. Effects similar to those reported here are likely to be important for ion-pair recombination in amorphous solids, for radical-pair reactions in single crystals, for electron-transfer reactions in rigid photosynthetic model systems, and possibly for radical-pair reactions on surfaces or in viscous organized media such as micelles, biological membranes, or polymers.

Acknowledgment. This work is supported by the NSF (PCM 7926677) and the Competitive Research Grants Office of the USDA (78-89-2066-01-147-1). C.E.D.C. is an NSF Predoctoral Fellow and S.G.B. is a Sloan and Dreyfus Fellow.

(4) $a(H)$ is independent of the angle between the electric polarization direction of the 532-nm exciting light and $\vec{H}$ to within the error limits.

(5) The magnetic field has no detectable effect on the detection system, and there is no evidence for alignment of the RCs in the magnetic field.

(6) Note that the relative yield is observed to saturate at very high field [i.e., the $I(H)$ curve levels off at high field in Figure 2A].

(7) (a) Chidsey, C. E. D.; Roelofs, M. G.; Boxer, S. G. *Chem. Phys. Lett.* **1980**, *74*, 113. (b) Boxer, S. G.; Chidsey, C. E. D.; Roelofs, M. G. J. *Am. Chem. Soc.* **1982**, *104*, 1452. This treatment is valid for the high-field limit, where the electron Zeeman interaction is much greater than the exchange, electron–electron dipolar, and nuclear hyperfine interactions, $H > 300$ G for RCs.

(8) Boxer, S. G.; Chidsey, C. E. D.; Roelofs, M. G. *Proc. Natl. Acad. Sci. U.S.A.*, in press. The isotropic g factor difference between $D^{+}\cdot$ and $A^{-}\cdot$ in RCs is about -1×10^{-3}.[7] The anisotropic quantum yield data at high field can be fit with a difference **g** tensor having principal values of -14×10^{-4}, -14×10^{-4}, and 1×10^{-4}, which is reasonable for aromatic radicals.

(9) See, for example: Turro, N. J.; Kraeutler, B. *Acc. Chem. Res.* **1980**, *13*, 369.

(10) See, for example: Lepley, A. R.; Closs, G. L., Eds. "Chemically Induced Magnetic Polarization"; Wiley: New York, 1973.

(11) The magnetic-field-dependent delayed fluorescence from single crystals due to an ion-pair reaction with dye molecules adsorbed on the surface exhibits an orientation dependence, which may be due to anisotropic magnetic interactions: Bube, W.; Michel-Beryerle, M. E.; Haberkorn, R.; Steffens, E. *Chem. Phys. Lett.* **1977**, *50*, 389.

Anionic Telomerization of Acrylonitrile Initiated by $^{-}CH_2CN$ in the Gas Phase

Richard N. McDonald* and A. Kasem Chowdhury

Department of Chemistry, Kansas State University
Manhattan, Kansas 66506

Received February 4, 1982

Although the kinetics and mechanism of free-radical-initiated polymerization processes of vinyl monomers have been reasonably understood for years, the same degree of understanding of ionic vinyl polymerization has not been achieved, primarily due to the lack of a method to observe the early stages of the ionic telomerization reaction. We report the first results of an anionic telomerization of a vinyl monomer in the gas phase, specifically acrylonitrile initiated by $^{-}CH_2CN$, where (a) the kinetics of the initiation and propagation steps leading to $NCCH_2-(CH_2CH(CN))_{-3}CH_2CHCN^{-}$ are determined and (b) under these conditions, the termination step of this "living" tetrameric anion is shown to depend on the structure of the anion initiator with intramolecular ion–dipole interactions reducing the reactivity of anionic end of this telomer.

Our approach to the study of gas-phase ionic telomerizations uses a flowing afterglow (FA) apparatus.[1] The initiator, $^{-}CH_2CN$ (m/z 40) was produced in the upstream end of the flow tube by the fast H^{+} transfer reaction[2] between H_2N^{-} and CH_3CN ($k = (4.5 \pm 0.3) \times 10^{-9}$ cm^3 molecule^{-1} s^{-1}) in helium as the buffer gas (P_{He} = 0.5 to 1.2 torr, flow velocity ($\bar{v}$) = 36 to 80 m s^{-1}). Some association of $^{-}CH_2CN$ with CH_3CN occurred to yield the cluster ion $NCCH_2^{-}(CH_3CN)$ (m/z 81). The chemically activated $^{-}CH_2CN$ ions are thermalized to their ground state by numerous collisions with the helium buffer gas in the flow tube prior to reaching the neutral reactant [N] addition port and the ion–molecule reaction commences. The ion composition of the flow is monitored with a quadrupole mass spectrometer as a function of added N. Rate constants (±30% accuracy) for the ion–molecule reactions are calculated by methods previously described.[1]

When $H_2C{=}CHCN$ was added to the helium flow (P_{He} = 1.1 torr, $\bar{v}$ = 36 m s^{-1}) containing anions m/z 40 and 81, the sequential production of the telomeric anions m/z 93, 146, 199, and 252 was observed (see Figure 1). The rate constants for the decay of m/z 40 and 81 ($\sim 6 \times 10^{-10}$ cm^3 molecule^{-1} s^{-1}) are the same as those

(1) McDonald, R. N.; Chowdhury, A, K.; Setser, D. W. *J. Am. Chem. Soc.* **1980**, *102*, 6491.

(2) Amide ion was produced by dissociative electron attachment to NH_3 at the electron gun.

0002-7863/82/1504-2675$01.25/0

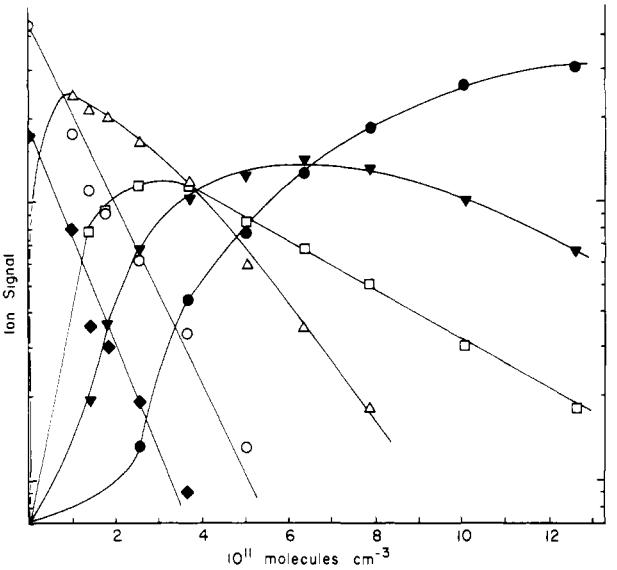

Figure 1. Semilog plot for the decay of $NCCH_2^-$ (m/z 40, ○) and $NCCH_2^-(CH_3CN)$ (m/z 81, ♦) and formation of the telomeric anions m/z 93 (△), 146 (□), 199 (▼), and 252 (●) for the reaction of m/z 40 and 81 with $H_2C{=}CHCN$ vs. added acrylonitrile.

measured at $P_{He} = 0.5$ torr, $\bar{v} = 80$ m s^{-1}, indicating no P_{He} dependence, at least at these extremes. Computer simulation of the data in Figure 1 gives a good fit with the rate constants given in eq 1–4.[3] The early maximum of the monomeric anion m/z

$$\underset{m/z\ 40}{NCCH_2^-} + H_2C{=}CHCN \rightarrow \underset{m/z\ 93}{NCCH_2{-}CH_2(CH{-}CN)^-} \quad (1)$$

$$k_{calcd} = 1.2 \times 10^{-9}\ cm^3\ molecule^{-1}\ s^{-1}$$

$$m/z\ 93 + H_2C{=}CHCN \rightarrow \underset{m/z\ 146}{NCCH_2{-}CH_2CH(CN){-}CH_2(CH{-}CN)^-} \quad (2)$$

$$k_{calcd} = 4.2 \times 10^{-10}\ cm^3\ molecule^{-1}\ s^{-1}$$

$$m/z\ 146 + H_2C{=}CHCN \rightarrow \underset{m/z\ 199}{NCCH_2{-}(CH_2CH(CN))_2{-}CH_2(CH{-}CN)^-} \quad (3)$$

$$k_{calcd} = 5 \times 10^{-10}\ cm^3\ molecule^{-1}\ s^{-1}$$

$$m/z\ 199 + H_2C{=}CHCN \rightarrow \underset{m/z\ 252}{NCCH_2{-}(CH_2CH(CN))_3{-}CH_2(CH{-}CN)^-} \quad (4)$$

$$k_{calcd} = 2.4 \times 10^{-10}\ cm^3\ molecule^{-1}\ s^{-1}$$

93 requires the total decay rate constant of the initiator anion(s) to be 1.2×10^{-9} cm^3 $molecule^{-1}$ s^{-1}. Although this is the sum of the individual decay rate constants for m/z 40 and 81, it is most likely that addition of m/z 40 to $H_2C{=}CHCN$ yielding m/z 93 successfully competes with clustering of m/z 40 with CH_3CN ($\rightarrow m/z$ 81) leading to decay of both m/z 40 and 81. Cluster formation between an anion and its conjugate acid generally reduces the rate constant of the clustered anion vs. that of the simple anion in nucleophilic reactions.[5]

From computer simulation, we should have been able to easily observe the pentameric anion (m/z 305) if the rate constant for its formation was $\geq 2 \times 10^{-11}$ cm^3 $molecule^{-1}$ s^{-1}. Two explanations can be offered for termination at the tetrameric species. First, an intramolecular Thorpe–Ziegler condensation[6] may occur as is reported in the condensed phase.[7] However, it is not clear why the condensation would be specific to the tetrameric anion; the dimeric and trimeric anions could yield six- or six- and eight-membered ring α-cyano iminoyl anions, respectively.

Alternatively, molecular models of the various telomeric anion products (eq 1–4) show that intramolecular ion–dipole interactions between the anion growing end, $-CHCN^-$, and *a single cyano group* on the telomer backbone are possible in the monomeric through trimeric anions. *The structure of the tetramer* (eq 4), however, *uniquely allows for two such interactions* (the cyano groups of the initiator and of the third monomer unit) *with the anion growing end*, with one cyano group above and the other below the plane of the $-CHCN^-$ group. This folded configuration can literally sandwich the anion growing end of the tetrameric species between dipolar cyano groups. Such an electrostatic interaction would stabilize the "living" telomer ionic end and sufficiently reduce its reactivity toward further addition with $H_2C{=}CHCN$ to terminate the telomerization under the present experimental conditions. Therefore, we suggest that this is the mechanism of termination of this reaction. This suggestion is substantiated by the fact that when CH_3O^- initiates the telomerization of $H_2C{=}CHCN$, sequential formation of the pentameric anion, $CH_3O{-}(CH_2CH(CN))_4CH_2CHCN^-$, is observed.[8]

This is only one of a variety of ionic telomerization reactions that can be studied in the gas phase and simply opens the door to this fascinating area of chemical research. We believe that a host of questions in polymer chemistry (mechanism, structure, reactivity, configurational effects, copolymerization, etc.) can be probed at these early mechanistic stages with this (FA) and other gas-phase methods.

Acknowledgment. We gratefully acknowledge support of this research from the U.S. Army Research Office and the National Science Foundation (equipment grant) and encouragement from and discussions with Professors D. W. Setser and H. K. Hall.

Registry No. $NCCH_2^-$, 21438-99-3; CH_3CN, 75-05-8; $H_2C{=}CHCN$, 107-13-1; 1,3,5,7,9-pentacyanononane anion, 81388-06-9.

(3) Michael (conjugate) addition reactions to $H_2C{=}CHCN$ have been previously reported with $c\text{-}C_5H_4^-$· and PhN^-· as the nucleophiles.[1,4]

(4) McDonald, R. N.; Chowdhury, A. K. *J. Am. Chem. Soc.* **1980**, *102*, 6146.

(5) Bohme, D. K.; Mackay, G. I. *J. Am. Chem. Soc.* **1981**, *103*, 978.

(6) See: March, J. "Advanced Organic Chemistry", 2nd ed.; McGraw-Hill: New York, 1977; p 873.

(7) Tsvetanov, C.; Panayotov, I. *Eur. Polym. J.* **1975**, *11*, 209.

(8) McDonald, R. N.; Chowdhury, A. K., unpublished results. The conjugate addition reaction of CH_3O^- with $H_2C{=}CHCN$ was a minor reaction channel; the major processes were H^+ transfer to give $C_3H_2N^-$ and formation of CN^-.